Feasibility analysis of a self-reinforcing electroadhesive rotational clutch

Detailleur, Alvaro; Umans, Sachin; Van Even, Herbert; Pennycott, Andrew; Vallery, Heike

Important note
To cite this publication, please use the final published version (if applicable).
Please check the document version above.

Feasibility Analysis of a Self-Reinforcing Electroadhesive Rotational Clutch

Alvaro Detailleur
Faculty of Mechanical, Maritime, and Materials Engineering
Delft University of Technology
Delft, The Netherlands
a.detailleur@student.tudelft.nl

Sachin Umans
Faculty of Mechanical, Maritime, and Materials Engineering
Delft University of Technology
Delft, The Netherlands
s.a.umans@student.tudelft.nl

Herbert Van Even
Faculty of Mechanical, Maritime, and Materials Engineering
Delft University of Technology
Delft, The Netherlands
h.j.l.vaneven@student.tudelft.nl

Andrew Pennycott
Faculty of Mechanical, Maritime, and Materials Engineering
Delft University of Technology
Delft, The Netherlands
a.pennycott@tudelft.nl

Heike Vallery
Faculty of Mechanical, Maritime and Materials Engineering
Delft University of Technology, Delft
& Department of Rehabilitation Medicine, Erasmus MC, Rotterdam
The Netherlands
h.vallery@tudelft.nl

Abstract—Building upon recent advancements in linear electroadhesive clutch materials and performance, this paper examines the feasibility of a self-reinforcing electroadhesive rotational clutch using a simple model. The design aims to deliver improvements in applications where performance is limited by the torque-to-power and torque-to-mass ratios offered by conventional electromagnetic or magnetorheological clutches. The performance of the self-reinforcing design is related to the device's geometric parameters and hence the robustness of clutch configurations is examined by modeling the system parameters as having stochastic properties. A design example based on the clutch requirements of a gyroscopic balance assistance device is analyzed. The analysis predicts that substantial improvements in torque-to-power and torque-to-mass ratios are possible with the presented design compared to industry-leading rotational clutches.

Index Terms—clutch, electroadhesion, self-reinforcing, wearable robotics

I. Introduction

Clutches are essential elements in a variety of mechatronic systems, for example in robotics [22]. The majority of current high-performance, electrically powered clutches rely on components such as solenoids or electromagnets that have high mass and power consumption [10].

A promising new development in the field of lightweight, high-performance clutches is the concept of electroadhesive clutches [2], [9], [23]. This type of clutch utilizes two opposing electroadhesive films, each consisting of an electrode covered in a thin layer of dielectric material with a high coefficient of friction. The dielectric material enables the electrodes to store a variable amount of electric charge, which can be used to generate a friction force between the two electrode surfaces to impede relative movement between the electrode surfaces.

Indicative tests of linear electroadhesive clutch prototypes show a strong reduction in power consumption and overall mass [10], [13], [25], [28]. This technology also holds promise for lightweight, high-performance rotational clutches for a variety of applications where power consumption and mass are still limiting factors, such as wearable robotics [11], [17].

However, simply extending the electrostatic adhesion to an axially symmetric shape would not result in improved holding torque per unit volume compared to current compact rotational clutches, as is shown in the Appendix.

To obtain electroadhesive rotational clutches with improved torque-to-mass and torque-to-volume ratios, and a holding torque similar to traditional clutches, we propose a design that amplifies the electroadhesive torque via self-reinforcement. The proposed principle utilizes the locking behavior of drum brakes previously explored in [3], [4], [20] and draws inspiration from the analysis presented in [16].

In Section II, we study the feasibility of the self-reinforcing design via a model that predicts the holding torque. Self-reinforcing designs are known to be sensitive to small perturbations [16]. Therefore, we optimize the geometry to find the least sensitive configuration. We also present a design example based on the theoretical requirements for a gyroscopic balance assistance device [14], [15], [18]. In Section III, the estimated performance of an electroadhesive clutch based on the proposed design is compared to SEPAC RFTC-320 electromagnetic clutches, which currently deliver industry-leading torque-to-mass and torque-to-power ratios [10], [24].

II. Methods

A. Proposed design

Similar to a drum brake, the design of Fig. 1(a) consists of two main parts. First, *the input drum*, a hollow cylinder constrained to rotate about its axis of symmetry, is considered the input of the clutch. A torque T is applied to this component.
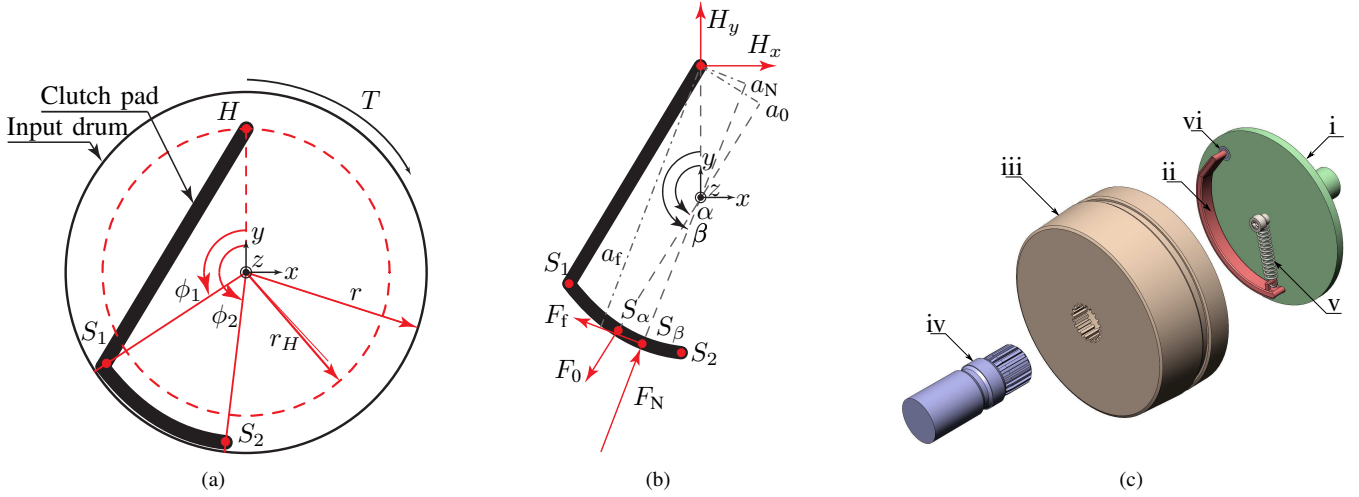
Fig. 1. (a) A schematic representation of the proposed design consisting of the input drum, visible as a circle, and the clutch pad, visible as a solid shape within the input drum. The variables and the Cartesian xyz coordinate system defined for analysis are also indicated. (b) A free-body diagram of the clutch pad. The coordinate system used is the same as in Fig. 1(a). (c) A CAD model of a possible design of the clutch concept: i) outgoing shaft, ii) clutch pad, iii) input drum, iv) incoming shaft, v) return spring, vi) hinge.

The inner surface of the drum is lined with an electroadhesive film. Second, *the clutch pad* resembles a brake pad of a drum brake. This component has a surface with the same radius of curvature as the input drum (S_1 to S_2). The side of the clutch pad facing the input drum is also lined with electroadhesive film, creating an interface similar to a linear electroadhesive clutch. The clutch pad is also attached to the output shaft of the clutch (not visible) via a hinge at point H. The design allows for multiple clutch pads inside the input drum.

The basic principle of this design mimics that of linear electroadhesive clutches. In the locked state, an opposing voltage is applied between (i) the electroadhesive film on the input drum and (ii) the electroadhesive film(s) on the clutch pad(s). This creates frictional forces at the drum-pad interface, which transmit a torque to the output shaft. In the unlocked state, no voltage is applied, allowing relative motion with minimal torque transfer. A restoring mechanism, e.g. spring or compliant mechanism, may be introduced to ensure the electroadhesive film surfaces are close enough to engage properly from the unlocked state and to physically disengage the electroadhesive films in the unlocked state.

If the applied torque is in the direction indicated by T in Fig. 1(a), particular geometries of the proposed design require a normal force greater than the electrostatic force generated by the electroadhesive films to maintain a moment balance around hinge point H. Thus, the design is capable of amplifying the maximum holding torque.

B. Model parameterization and assumptions

Self-reinforcing and self-energizing clutches exhibit different properties [16]. In the former type, the amplification of the holding torque results in a finite maximum holding torque, whereas in the latter type, if the coefficient of friction is assumed constant, the holding torque is theoretically infinite, even for (infinitesimally) small input forces. To ensure that no torque is transmitted when the clutch is in its unlocked state, we consider only self-reinforcing designs.

A particular clutch configuration is characterized by five parameters (Fig. 1(a)):

- r, the radius of the input drum.
- r_H, the radius of the hinge point H with respect to the center of the input drum.
- ϕ_1, the starting angle of the electroadhesive film on the clutch pad relative to the hinge H, defining point S_1.
- ϕ_2, the end angle of the electroadhesive film on the clutch pad with respect to H, defining point S_2.
- d, the depth of the device along the z-axis.

To determine the maximum holding torque, the forces on the clutch pad are examined via a free-body diagram (Fig. 1(b)). Throughout the analysis, gravitational and centrifugal effects, and forces of mechanisms used to ensure proper engagement of the electroadhesive films will be neglected. In addition, the following assumptions regarding the distribution and points of force application (Fig. 1(b)) are made:

The electrostatic force, F_0, resulting from the opposing charge stored in the electroadhesive films, is assumed to have a uniform distribution along the drum-pad interface. Hence, the resultant force acts at the middle of the electroadhesive lining at angle $\alpha = \frac{1}{2}(\phi_1 + \phi_2)$ relative to hinge point H. S_α denotes the point of application of this force.

The resultant normal force F_N, which the input drum exerts on the clutch pad in radial direction, is modeled as in brake pads of drum brakes. It is assumed the brake lining is the only body being deformed, which leads to a sinusoidal distribution of the normal force along the brake pad [4], [21]. Therefore, the resultant normal force acts at S_β, at a relative angle to point H approximated by

$$\beta = \frac{\sin(\phi_2) - \sin(\phi_1) + \phi_1 \cos(\phi_1) - \phi_2 \cos(\phi_2)}{\cos(\phi_1) - \cos(\phi_2)}. \quad (1)$$

The friction force, F_f, resists relative movement between the input drum and clutch pad, and is assumed to act perpendicularly to the resultant normal force F_N. An upper bound on its magnitude follows from Coulomb's law of friction [6], [10], [13]. The coefficient of friction is denoted by μ_f.

The constraining force from the hinge of the clutch pad is decomposed into components H_x and H_y acting in the direction of the x and y-axis, respectively. It is assumed that the hinge does not exert any moment on the clutch pad.

C. Relation between parameters and amplification factor

To characterize the amplification of the nominal friction force produced, we define the amplification factor ξ as the ratio between F_N and F_0. In static equilibrium, the moments of the three forces F_N, F_0, and F_f must be in moment balance with respect to point H:

$$\sum M_H = a_N F_N - a_0 F_0 - a_f F_f = 0, \tag{2}$$

with the scalar moment arms a_N, a_0, and a_f. So, ξ is

$$\xi = \frac{F_N}{F_0} = \frac{\frac{a_0}{a_N}}{1 - \frac{a_f}{a_N} \cdot \frac{F_f}{F_N}}. \tag{3}$$

We define the parameters q_1 and q_2 as the ratios $q_1 = \frac{a_0}{a_N}$ and $q_2 = \frac{a_f}{a_N}$, respectively. The condition for self-reinforcing behavior is then found by examining the denominator of Equation (3) for the limiting case: $|\mu_f q_2| < 1$. If $|\mu_f q_2| \geq 1$, the clutch design is self-energizing, which is undesired.

D. Calculation of the required amplification factor

Given a target holding torque, electroadhesive film material properties and constraints on the allowable physical dimensions, the required amplification factor can be determined.

The magnitude of the holding torque T results from:

$$T = |F_f|\, r \leq \mu_f \xi |F_0| r. \tag{4}$$

Next, given the coefficient of friction, μ_f, the maximum shear pressure, τ, that the electroadhesive film is capable of producing *without* amplification and the area lined with electroadhesive film A, the norm of the achievable electrostatic force $|F_0|$ can be estimated via

$$|F_0| = \frac{\tau A}{\mu_f}, \tag{5}$$

and the required amplification factor results from (4) and (5):

$$\xi = \frac{T}{\tau A r}. \tag{6}$$

If the assumption is made that the design utilizes multiple clutch pads covering a fraction ζ of the inner surface area of the drum, then A may be set to equal $2\pi \zeta r d$ and hence

$$\xi = \frac{T}{2\pi \zeta \tau r^2 d}. \tag{7}$$

The remainder of the inner surface area of the drum, $1 - \zeta$, is reserved to ensure the design can be physically realized.

E. Determining the most robust clutch configuration

To quantify the robustness of clutch configurations with respect to (small) perturbations, a sensitivity analysis is performed on the amplification factor, ξ. In addition to the inherent sensitivity of self-reinforcing designs to perturbations, the performance and failure mechanisms of electroadhesive clutches are not yet fully understood [6], [10]. Therefore, the expected performance of these devices is subject to a large degree of uncertainty, motivating the proposed analysis.

The geometric description of clutch configurations is simplified by introducing the dimensionless variable $r_{\text{frac}} = \frac{r_H}{r}$. In addition, the parameter space $P \subset \mathbb{R}^4$ is introduced. Each point $\vec{p} = [\mu_f, \phi_1, \phi_2, r_{\text{frac}}]^T \in P$ uniquely defines a physically realizable clutch configuration.

Letting p_i denote the i-th element of vector $\vec{p}$, the parameter space is formally defined as

$$P = \{\vec{p} \in \mathbb{R}^4 \mid p_1 \geq 0,\, 0 < p_2 < p_3 < \pi, 0 < p_4 < 1\}. \tag{8}$$

Additional constraints may be introduced, such as setting the coefficient of friction equal to that of a specific dielectric film, requiring the clutch geometry to achieve a certain (minimum) degree of self-reinforcement or selecting only geometries with a (minimum) difference between ϕ_1 and ϕ_2. To ensure that multiple clutch pads maximize the interface area with the input drum, this difference may be set to equal $\frac{2\pi}{k}$ with $k \in \mathbb{N}_{>0}$.

The perturbations which a clutch configuration experiences are modeled by assuming the friction coefficient μ_f and the arms a_0, a_N and a_f have stochastic properties. For this reason, the vector of random variables $\vec{X} = [M, A_0, A_N, A_f]^T$ is introduced, which represents a perturbed clutch configuration. These variables are assumed to be independent and identically distributed random variables (i.i.d.) with a multi-variate Gaussian distribution. The expected value $\vec{\mu}_X$ corresponds to the nominal design values,

$$\vec{\mu}_X = [p_1, a_0(\vec{p}), a_N(\vec{p}), a_f(\vec{p})]^T. \tag{9}$$

The covariance matrix $\boldsymbol{\Sigma}_X$ is determined by assuming that $\pm 10\%$ of $\vec{\mu}_X$ corresponds to a three-sigma interval:

$$\boldsymbol{\Sigma}_X = \left(\frac{0.1}{3}\right)^2 \cdot \text{diag}\left(\mu_{X_1}^2, \mu_{X_2}^2, \mu_{X_3}^2, \mu_{X_4}^2\right). \tag{10}$$

Next, the function $f \colon P \mapsto \mathbb{R}$ is introduced, which maps the parameter space to the corresponding amplification factor space. Defining the vector $\vec{Y} = f(\vec{X})$, the metric quantifying the sensitivity of a configuration $\vec{p}$ is the covariance matrix $\boldsymbol{\Sigma}_Y$ of $\vec{Y}$. Expressing $\boldsymbol{\Sigma}_Y$ in terms of the geometric variables of $\vec{p}$ allows (geometric) constraints to be readily taken into account in the optimization problem.

Overall, the constrained optimization problem of finding a minimally sensitive clutch configuration can be stated as:

$$\vec{p}^* = \underset{\vec{\mu}_X \in P}{\arg\min}\ \boldsymbol{\Sigma}_Y. \tag{11}$$

Due to the nonlinear nature of f, Equation (11) cannot easily be solved. To determine a minimally sensitive configuration, the nonlinear function f is approximated by a

Taylor expansion. Let T_1 and T_2 denote the first- and second-order multivariate Taylor approximations of f. Furthermore, following the convention in [12], utilize index notation to reference (i) the i-th expression of the vector-valued function f as f_i and (ii) a matrix of which the (i,j) element is $[A_{ij}]_{ij}$. Then, the variance $\mathbf{\Sigma}_{T_1}$ of T_1 is given by

$$\mathbf{\Sigma}_{T_1} = f'(\vec{\mu}_X)\mathbf{\Sigma}_X f'(\vec{\mu}_X)^{\mathrm{T}}, \tag{12}$$

and the variance $\mathbf{\Sigma}_{T_2}$ of T_2 is

$$\mathbf{\Sigma}_{T_2} = \mathbf{\Sigma}_{T_1} + \frac{1}{2}\left[\mathrm{tr}\left(\mathbf{\Sigma}_X f_i''(\vec{\mu}_X)\mathbf{\Sigma}_X f_j''(\vec{\mu}_X)\right)\right]_{ij}. \tag{13}$$

Equation (13) can be used to approximate $\mathbf{\Sigma}_Y$. Using established solvers for constrained optimization problems, an approximate solution is found by minimizing $\mathbf{\Sigma}_{T_2}$.

The accuracy of the approximation is quantified via a Monte Carlo simulation for a configuration found to be optimal. The sample variance estimator is then used to determine the value of $\mathbf{\Sigma}_Y$ and its deviation from $\mathbf{\Sigma}_{T_2}$.

F. Design example: Safety clutch for a wearable gyroscopic balance assistance device

We investigate a possible application of the proposed clutch design in a wearable balance assistance device, as previously described in [14], [15]. This device contains gyroscopic actuators in a backpack-like construction. The actuation principle relies on fast-spinning wheels that are gimbaled. When an actuator rotates the gimbal, the angular momentum of the wheels changes, exerting a reaction torque on wearers to help them maintain their balance. One realization of such a wearable gyroscope incorporates an additional, passive gimbal [18], which can in principle decouple the gyroscopic moment from the user, mainly for safety reasons. This decoupling requires a controllable clutch with low mass and volume.

For the envisioned use case, allowable values for r and d are approximately $0.06\,\mathrm{m}$ and $0.05\,\mathrm{m}$, respectively. The clutch is expected to work in both directions using a mirror-symmetric configuration of pads. This means each pad uses only half of the axial dimension d i.e. $0.025\,\mathrm{m}$. For each direction, only the holding torque produced by clutch pads amplifying the torque is considered. This is a conservative estimate, as the opposing clutch pads also contribute to the holding torque. A $35\,\mathrm{N\,m}$ holding torque is to be achieved [15], [18].

The coefficient of friction $\mu_{\mathrm{f}} = 0.63$ and the maximum, non-amplified shear pressure $\tau = 23\,\mathrm{kPa}$ are taken from [10]. Estimating $\zeta = 0.9$ and evaluating Equation (7) with these parameters returns $\xi \approx 2.99$, which is incorporated as an additional constraint in the optimization. Furthermore, a minimum clutch pad arc of $\phi_2 - \phi_1 = \frac{2\pi}{10}$ is enforced, and the maximum value of r_{frac} is set at 0.925 in order to ensure the hinge position can be physically realized. Within the context of this example, we define the parameter space of clutch configurations meeting all of the above criteria as P^+.

G. Implementation of the sensitivity analysis

The sensitivity analysis is performed to find a minimally sensitive clutch configuration within the constrained parameter space P^+. The coefficient of friction of the dielectric material determines p_1. In addition, the value of amplification factor ζ is specified to be 2.99. Therefore, assuming none of the inequalities within this space are active, the solution space consists of a two-dimensional manifold.

The constrained optimization problem is solved with the second-order Taylor approximation $\mathbf{\Sigma}_{T_2}$ using the *fmincon* function in MATLAB. The interior-point algorithm, which is applied to solve linear and nonlinear convex optimisation problems with inequality constraints [8], was used with the constraint, step and optimality tolerances set to 10^{-10}. Other options were left at default values. The MATLAB script used to perform the optimization is available in the 4TU.ResearchData repository [7].

As a validation of the second-order approximation, a Monte Carlo analysis of $N = 10^6$ points is performed on the optimal clutch configuration.

H. Performance comparison

The expected performance of the optimal clutch configuration is compared to that of an industry-leading SEPAC RFTC-320 electromagnetic clutch [10], [24]. A comparison is made between the (i) holding torque, (ii) volume, (iii) power consumption and (iv) mass. The power consumption and mass are estimated using the data and design example in [10].

III. RESULTS

A. Sensitivity analysis

The second-order approximated variance, $\mathbf{\Sigma}_{T_2}$, and optimal geometry $\vec{p}_{T_2}$, are 0.1704 and $[0.63,\ 1.2207,\ 1.8490,\ 0.925]^{\mathrm{T}}$, respectively. The sample variance of the Monte Carlo simulation on $\vec{p}_{T_2}$, $\mathbf{\Sigma}_{\mathrm{MC}} = 0.1932$, differs by approximately 13% from the approximation of $\mathbf{\Sigma}_{T_2}$. For the configuration of $\vec{p}_{T_2}$, both the inequalities on $\phi_2 - \phi_1$ and r_{frac} are active.

The value of $\mathbf{\Sigma}_{T_1}$ over P^+ is shown in Fig. 2. In addition, the constraints $r_{\mathrm{frac}} \leq 0.925$ and $\phi_2 - \phi_1 \geq \frac{2\pi}{10}$, and the solution $\vec{p}_{T_2}$ are visualized. The figure illustrates that the objective function gradient with respect to ϕ_1 and ϕ_2 is shallow near the optimal solution.

B. Performance comparison

A comparison between the optimal electroadhesive clutch from the design example and the benchmark SEPAC RFTC-320 clutch [24] is tabulated in Table I. The estimated mass of all electroadhesive films and supporting electronics is $0.04\,\mathrm{kg}$. However, the total clutch mass cannot be accurately estimated for the current conceptual design.

IV. DISCUSSION

A. Validation of sensitivity analysis

The value of $\mathbf{\Sigma}_{T_2}$ differs approximately 13% from the value obtained from the Monte Carlo simulation, $\mathbf{\Sigma}_{\mathrm{MC}}$. The difference between these two values is sufficiently small and
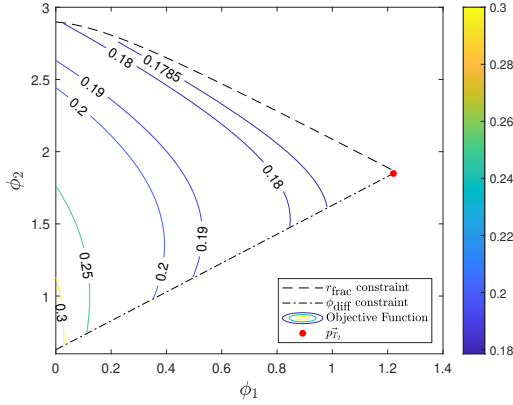
Fig. 2. Contour plot of the objective function for the first-order Taylor approximation over P^+. The red marker indicates the minimally sensitive configuration $\vec{p}_{T_2}$.
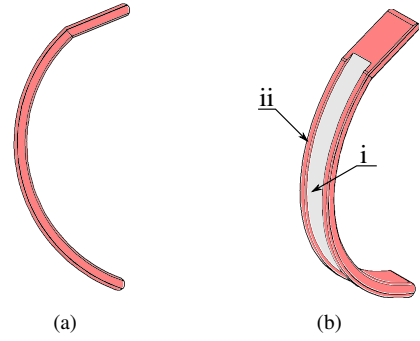

Fig. 3. Impression of a possible wear-resistant clutch pad. (a) side profile showing curvature, (b) isometric view showing the groove with the dielectric material (i) and sacrificial material (ii).

TABLE I
COMPARISON BETWEEN DESIGN EXAMPLE AND BENCHMARK CLUTCH.

	Proposed clutch	SEPAC clutch
Holding torque (Nm)	35*	54
Volume (m^3)	$5.65 \cdot 10^{-4}$	$5.34 \cdot 10^{-4}$
Power (W)	$6.6 \cdot 10^{-3}$	$24 - 33$
Mass (kg)	Specific to design	0.91

*: Conservative estimate neglecting contribution of opposing clutch pads.

therefore the second-order Taylor expansion is deemed a good approximation of f for the sensitivity metric Σ_Y.

A Monte Carlo analysis performed on the configuration $\vec{p}_{T_1}$, obtained by approximating Σ_Y using Σ_{T_1}, indicated this geometry was more sensitive to perturbations. This justifies the second-order approximation of the sensitivity metric.

B. Comparison to SEPAC RFTC-320

Table I indicates that the estimated clutch performance from the design example is comparable to the benchmark SEPAC RFTC-320 clutch and even exceeds it in certain respects. The performed analysis shows favorable self-reinforcing characteristics are possible while obtaining torque-to-volume ratios similar to the benchmark clutch. In addition, marked improvements in power consumption and mass are expected for this design, as it does not require heavy, power-consuming components such as electromagnets and solenoids. Fig. 1(c) shows a possible practical design for the clutch concept.

C. Practical limitations regarding wear

When engaging the clutch, sliding will inevitably occur between the dielectric layers of the input drum and clutch pad. This sliding will result in friction and wear, which is defined as damage due to the removal of surface material and may result from abrasive, thermal and fatigue-related factors [26].

The material used in [10] is barium titanate (BaTiO$_3$) [17]. This has a Vickers hardness of 418 HV, which is comparable to glass and is indicative of good wear resistance [1], [19]. This is further reinforced by the fact that the stress the normal force exerts on the dielectric surfaces is far below the failure stress of BaTiO$_3$. Experiments investigating self-mated sliding between ceramics similar to BaTiO$_3$ found a volumetric wear coefficient k of 10^{-15} to $10^{-14}\,\mathrm{N/m^3}$, which represents mild wear [5], [27].

An estimate of the layer height h_i that is stripped away each time the clutch is engaged is made using the Archard equation [5], $h_i = kPs_i$, where k is the volumetric wear coefficient, P the pressure on the clutch pad and s_i the sliding distance of the clutch pad on the input drum surface per activation of the clutch. Using the aforementioned value of $10^{-14}\,\mathrm{N/m^3}$ for k, calculating $P = \frac{\tau\xi}{\mu_\mathrm{f}} = 109\,\mathrm{kPa}$ for the clutch configuration $\vec{p}_{T_2}$ of the design example and assuming a value of $5 \times 10^{-3}\,\mathrm{m}$ for s_i, we estimate the clutch can be engaged in the order of magnitude of 10^6 times before a dielectric layer of $60\,\mu\mathrm{m}$ is stripped away. This layer thickness is representative of the design presented in [10].

To vary μ_f and protect the dielectric material, the electroadhesive film could be placed in a groove such that the top dielectric layer is lower than the surface of the clutch pad. When the clutch is engaged, this layer of "sacrificial" material slides and experiences wear first, instead of the dielectric layer. Fig. 3 shows a design with such a groove.

D. Advice concerning the choice of parameters

Configurations with lower amplification factors exhibit more stable behavior [16]. Therefore, within the geometrical constraints, r^2, d and ζ should be maximized to minimize the required amplification factor ξ.

E. Directions for future research

Further research should be performed to be able to better predict clutch performance and self-reinforcing behavior. First, further testing should be performed on the electroadhesive film to determine uniformity of the force distribution. As the dielectric material is resistant to deformation, this assumption is expected to be relatively accurate [10]. Second, the normal force distribution should be determined more accurately than the current sinusoidal approximation, for example, using a Finite Element Method analysis. Finally, a prototype of the clutch could be built according to the optimal configuration

presented in this paper. The prototype's performance should be analyzed and compared to the presented model predictions.

V. Conclusion

This paper shows the conceptual feasibility of a clutch design combining the principles of self-reinforcing brakes with electroadhesive film materials. Given the modeling assumptions made, the design seems capable of achieving torque-to-volume ratios comparable to industry-leading, commercially available clutches [24]. In addition, substantial improvements in torque-to-power and torque-to-mass ratios seem possible due to the utilization of electroadhesive film material.

Acknowledgment

References

[1] M. Ashby, *Materials: engineering science, processing and design*. The Boulevard, Langeford Lange, Kindlington, Oxford, OX5, 1GB, IK: Elsevier, 2014.

[2] D. M. Aukes, B. Heyneman, J. Ulmen, H. Stuart, M. R. Cutkosky, S. Kim, P. Garcia, and A. Edsinger, "Design and testing of a selectively compliant underactuated hand," *The International Journal of Robotics Research*, vol. 33, no. 5, pp. 721–735, 2014.

[3] L. Balogh, T. Stréli, H. Németh, and L. Palkovics, "Modelling and simulating of self-energizing brake system," *Vehicle System Dynamics*, vol. 44, no. sup1, pp. 368–377, 2006.

[4] Z. Barecki and S. F. Scieszka, "A mathematical model of the brake shoe and the brake path system," *N&O Joernaal*, pp. 13–17, 1987.

[5] A. V. Beek, *Advanced Engineering Design*. TU Delft, 2015.

[6] A. S. Chen and S. Bergbreiter, "A comparison of critical shear force in low-voltage, all-polymer electroadhesives to a basic friction model," *Smart Materials and Structures*, vol. 26, no. 2, p. 025028, 2017.

[7] A. Detailleur and S. Umans, "constrained optimization script," may 2021. [Online]. Available: https://doi.org/10.4121/14579175

[8] I. Dikin, "Iterative solution of problems of linear and quadratic programming," in *Doklady Akademii Nauk*, vol. 174, no. 4. Russian Academy of Sciences, 1967, pp. 747–748.

[9] S. Diller, C. Majidi, and S. H. Collins, "A lightweight, low-power electroadhesive clutch and spring for exoskeleton actuation," in *2016 IEEE International Conference on Robotics and Automation (ICRA)*. IEEE, 2016. [Online]. Available: https://doi.org/10.1109/icra.2016.7487194

[10] S. B. Diller, S. H. Collins, and C. Majidi, "The effects of electroadhesive clutch design parameters on performance characteristics," *Journal of Intelligent Material Systems and Structures*, vol. 29, no. 19, pp. 3804–3828, 2018. [Online]. Available: https://doi.org/10.1177/1045389x18799474

[11] ESTAT Actuation, feb 2021. [Online]. Available: https://www.estat.tech/

[12] G. Hendeby and F. Gustafsson, "On nonlinear transformations of stochastic variables and its application to nonlinear filtering," in *International Conference on Acoustics, Speech, and Signal Processing (ICASSP)*, 2008.

[13] R. Hinchet and H. Shea, "High force density textile electrostatic clutch," *Advanced Materials Technologies*, vol. 5, no. 4, p. 1900895, 2020.

[14] D. Lemus, A. Berry, S. Jabeen, C. Jayaraman, K. Hohl, F. C. van der Helm, A. Jayaraman, and H. Vallery, "Controller synthesis and clinical exploration of wearable gyroscopic actuators to support human balance," *Scientific Reports*, vol. 10, no. 1, pp. 1–15, 2020.

[15] D. Lemus, J. van Frankenhuyzen, and H. Vallery, "Design and evaluation of a balance assistance control moment gyroscope," *Journal of Mechanisms and Robotics*, vol. 9, no. 5, p. 051007, 2017. [Online]. Available: https://doi.org/10.1115/1.4037255

[16] M. Liermann, "Self-energizing electro hydraulic brake," Ph.D. dissertation, RWTH Aachen, 2008.

[17] C. Majidi, S. Collins, and S. Diller, "Electrostatic clutch," U.S. Patent US10 355 624B2, 2020.

[18] C. Marquardt, D. Lemus, C. Meijneke, and H. Vallery, "Design and evaluation of series-elastic gyroscopic actuator for balance assistance," in *unpublished*, 2021.

[19] Michael Ashby, "CES Edupack database," Cambridge, 2020.

[20] D. Moschella, G. Gatti, E. Vitelli, A. Lecce, M. Perrelli, C. Pace, and G. A. Danieli, "Experimental validation of a special locking drum brake for robotic applications," in *Volume 4: Fatigue and Fracture; Fluids Engineering; Heat Transfer; Mechatronics; Micro and Nano Technology; Optical Engineering; Robotics; Systems Engineering; Industrial Applications*. ASMEDC, 2008.

[21] W. C. Orthwein, *Clutches and Brakes: Design and Selection*. Marcel Dekker Inc., 2004, ch. 3, pp. 31 – 34.

[22] M. Plooij, G. Mathijssen, P. Cherelle, D. Lefeber, and B. Vanderborght, "Lock your robot: A review of locking devices in robotics," *IEEE Robotics & Automation Magazine*, vol. 22, no. 1, pp. 106–117, 2015.

[23] V. Ramachandran, J. Shintake, and D. Floreano, "All-fabric wearable electroadhesive clutch," *Advanced Materials Technologies*, vol. 4, no. 2, p. 1800313, 2018. [Online]. Available: https://doi.org/10.1002/admt.201800313

[24] *SEPAC Data Sheet RFTC-320 Clutch*, SEPAC Inc., 2019. [Online]. Available: https://sepac.com/products/view/rotating-field-tooth-clutch/

[25] O. Testoni, A. Bergamini, S. Bodkhe, and P. Ermanni, "A novel concept for adaptive friction damper based on electrostatic adhesion," *Smart Materials and Structures*, vol. 29, no. 10, p. 105032, 2020.

[26] M. Watson, C. Byington, D. Edwards, and S. Amin, "Dynamic modeling and wear-based remaining useful life prediction of high power clutch systems," *Tribology Transactions*, vol. 48, no. 2, pp. 208–217, 2005.

[27] M. Woydt, A. Skopp, and R. Wäsche, "Ceramic-ceramic composite materials with improved friction and wear properties," in *4th International Symposium on Ceramic Materials and Components for Engines*. Springer Netherlands, 1992, pp. 1219–1239. [Online]. Available: https://doi.org/10.1007/978-94-011-2882-7_138

[28] K. Zhang, E. J. Gonzalez, J. Guo, and S. Follmer, "Design and analysis of high-resolution electrostatic adhesive brakes towards static refreshable 2.5d tactile shape display," *IEEE Transactions on Haptics*, vol. 12, no. 4, pp. 470–482, 2019.

Appendix

Here, we show that the torque-to-volume ratio of electroadhesive rotational clutches is independent of shape. We assume that rotational clutches utilizing electroadhesion have an axially symmetric shape lined with an electroadhesive film. The x-axis represents this axis of symmetry; the clutch has a length L along this axis, and a function $r(x)$ denotes the radius of the clutch shape along the axis of symmetry.

The torque $\mathrm{d}T$ produced by an infinitesimally small element of this rotationally symmetric shape depends on the increment $\mathrm{d}x$ along the x-axis, the radius $r(x)$ and the shear pressure τ of the electroadhesive material. Denoting $\mathrm{d}A(x) = 2\pi r(x)\,\mathrm{d}x$ and $\mathrm{d}V(x) = \pi r(x)^2\,\mathrm{d}x$ as the area and volume of the infinitesimal element at x, respectively, the total torque T and volume V of the shape are given by

$$T = \int_0^L \mathrm{d}T = \int_0^L \tau r(x)\,\mathrm{d}A(x) = 2\tau\,\pi \int_0^L r(x)^2\,\mathrm{d}x \quad (14)$$

and

$$V = \int_0^L \mathrm{d}V = \pi \int_0^L r(x)^2\,\mathrm{d}x. \quad (15)$$

The torque-to-volume ratio T/V follows from Equations (14) and (15). It is evident that the torque-to-volume ratio of all axially symmetric, electroadhesive rotational clutches is constant and equal to 2τ, irrespective of $r(x)$. For current electroadhesive films, the shear pressure τ is not sufficiently large to exceed the torque-to-volume ratio of state-of-the-art compact rotational clutches.